Phosphorus–carbon bond cleavage at a di-iron centre: synthesis of μ-phosphidomethyl complexes $[Fe_2(CO)_6(\mu\text{-}CH_2PR_2)(\mu\text{-}PR_2)]$ from $[Fe_2(CO)_6(\mu\text{-}CO)(\mu\text{-}R_2PCH_2PR_2)]$

Nancy M. Doherty, Graeme Hogarth, Selby A. R. Knox*, Kirsty A. Macpherson, Frauke Melchior, David A. V. Morton and A. Guy Orpen*

School of Chemistry, The University, Bristol BS8 1TS (UK)

Abstract

Upon heating in toluene at reflux the di-iron heptacarbonyl complexes $[Fe_2(CO)_6(\mu\text{-}CO)(\mu\text{-}R_2PCH_2PR_2)]$ (R = Ph, Me, Et, ^{i}Pr, OEt) lose carbon monoxide, resulting in phosphorus–methylene bond cleavage to give the μ-phosphidomethyl complexes $[Fe_2(CO)_6(\mu\text{-}CH_2PR_2)(\mu\text{-}PR_2)]$. The ability of the phenyl group to stabilise the μ-CH_2PR_2 ligand is seen in the thermolyses of the diphosphine complex $[Fe_2(CO)_6(\mu\text{-}CO)(\mu\text{-}Ph_2PCH_2PMe_2)]$, which undergoes selective Me_2P–CH_2 bond cleavage to yield $[Fe_2(CO)_6(\mu\text{-}CH_2PPh_2)(\mu\text{-}PMe_2)]$, and of the bis-diphosphine complexes $[Fe_2(CO)_4(\mu\text{-}CO)(\mu\text{-}R_2PCH_2PR_2)(\mu\text{-}Ph_2PCH_2PPh_2)]$ (R = Ph, Me), which results only in Ph_2P–CH_2 bond cleavage to give $[Fe_2(CO)_4(\mu\text{-}R_2PCH_2PR_2)(\mu\text{-}CH_2PPh_2)(\mu\text{-}PPh_2)]$. The ubiquity of μ-CH_2PPh_2 is attributed to the existence of a zwitterionic form in which positive charge residing on phosphorus is dispersed into the phenyl rings. The complexes $[Fe_2(CO)_4(\mu\text{-}R_2PCH_2PR_2)(\mu\text{-}CH_2PPh_2)(\mu\text{-}PPh_2)]$ exist as mixtures of geometric isomers **a** and **b**, identified by ^{31}P NMR spectroscopy and an X-ray diffraction study on the major isomer **a** of $[Fe_2(CO)_4(\mu\text{-}Me_2PCH_2PMe_2)(\mu\text{-}CH_2PPh_2)(\mu\text{-}PPh_2)]$ as its dichloromethane solvate, which contains a *cis* arrangement of phosphido and phosphidomethyl ligands with the diphosphine lying *trans* to the latter. Methyl substitution in the diphosphine backbone suppresses phosphorus–methylene bond cleavage and results instead in *ortho*-metalation and phosphorus–phenyl bond cleavage. Thus, on heating $[Fe_2(CO)_6(\mu\text{-}CO)\{\mu\text{-}Ph_2PCH(Me)(PPh_2\}]$ carbon monoxide and benzene are lost and $[Fe_2(CO)_6\{\mu\text{-}PhPCH(Me)P(Ph)(C_6H_4\text{-}o)\}]$ is formed, structurally characterised by X-ray diffraction. Substitution of two methyl groups into the diphosphine backbone favours *ortho*-metalation more strongly still and UV irradiation of the chelate complex $[Fe(CO)_3\{\eta^2\text{-}Ph_2PC(Me_2)PPh_2\}]$ in the presence of iron pentacarbonyl yields $[Fe_2(CO)_6\{\mu\text{-}PhPC(Me_2)P(Ph)(C_6H_4\text{-}o)\}]$ directly. The structure of $[Fe_2(CO)_6(\mu\text{-}CO)\{\mu\text{-}Ph_2PCH(Me)PPh_2\}]$ as its hexane solvate was examined by X-ray diffraction, for comparison with that of $[Fe_2(CO)_6(\mu\text{-}CO)\{\mu\text{-}Ph_2PCH_2PPh_2\}]$. The structure analysis was not satisfactory but no significant differences between the molecular structures were observed. The suppression of backbone P–C cleavage by methyl substitution is attributed to the destabilisation of the zwitterionic form of μ-CR_2PPh_2, which has negative charge residing on the carbon.

Introduction

In recent years we have carried out an extensive study of the organic chemistry of the diruthenium centre, based on the complex $[Ru_2(CO)_4(\eta\text{-}C_5H_5)_2]$ [1]. The iron carbonyl $[Fe_2(CO)_9]$ represented in principle an attractive complex for an extension of these studies to the di-iron centre, but it is notoriously prone to fragment to mononuclear species. However, diphosphine-bridged derivatives such as $[Fe_2(CO)_6(\mu\text{-}CO)(\mu\text{-}R_2PCH_2PR_2)]$ were known [2–9] and the effect of these ligands in stabilising dinuclear metal centres is well established [10, 11]; this approach has recently been used to stabilise thermally unstable $[Ru_2(CO)_9]$ [12]. A significant organic chemistry of the di-iron centre can indeed be developed from the species $[Fe_2(CO)_6(\mu\text{-}CO)(\mu\text{-}R_2PCH_2PR_2)]$, some aspects of which have been described [13–16], but we have also discovered that the complexes undergo an unprecedented phosphorus–carbon bond cleavage reaction on heating to give $[Fe_2(CO)_6(\mu\text{-}CH_2PPh_2)(\mu\text{-}PPh_2)]$, containing coordinated μ-phosphidomethyl and μ-phosphido moieties. Since synthetic routes to phosphidomethyl ligands are limited and the phosphorus–carbon bond cleavage process is recognised as a major deactivation pathway for phosphine complexes used as homogeneous catalysts [17], a study of this reaction has been carried out and is described here. Aspects of the work have appeared as a preliminary communication [18].

*Authors to whom correspondence should be addressed.

0020-1693/92/$5.00

Results and discussion

Synthesis and characterisation of $[Fe_2(CO)_6(\mu\text{-}CO)(\mu\text{-}R_2PXPR'_2)]$ (1–6)

Cotton and Troup first described the synthesis of a diphosphine-bridged derivative of $[Fe_2(CO)_9]$, the complex $[Fe_2(CO)_6(\mu\text{-}CO)(\mu\text{-}Ph_2PCH_2PPh_2)]$ (**1**) being obtained in 56% yield by the room temperature reaction of the carbonyl and bis(diphenylphosphino)methane (dppm) in tetrahydrofuran [2]. In our hands, however, this method led to the isolation of **1** in only 15–25% yield, tedious chromatography being required to remove the other products, namely $[Fe(CO)_4(\eta^1\text{-dppm})]$ [3] $[Fe(CO)_3(\eta^2\text{-dppm})]$ [19] and the non-metal–metal bonded $[Fe_2(CO)_8(\mu\text{-dppm})]$ [3]. Since Wegner *et al.* had reported [3] that the UV irradiation of $[Fe_2(CO)_8(\mu\text{-dppm})]$ leads to quantitative formation of **1** and we had previously observed [20] that irradiation of $[Fe(CO)_4(\eta^1\text{-dppm})]$ or $[Fe(CO)_3(\eta^2\text{-dppm})]$ in the presence of an excess of iron pentacarbonyl resulted in the high yield formation of **1**, it was clear how the original synthesis might be improved: addition of $[Fe(CO)_5]$ and extended irradiation should convert the three side-products to **1**. This proved to be the case. Thus, after reaction of dppm with a slight excess of $[Fe_2(CO)_9]$ in thf for 2 h an excess of iron pentacarbonyl was added and the mixture subjected to UV irradiation for 16 h, giving **1** in 95% yield after chromatography. In a similar way, the analogues $[Fe_2(CO)_6(\mu\text{-}CO)(\mu\text{-}R_2PCH_2PR'_2)]$ (**2–6**) were prepared from the appropriate diphosphine in 45–95% yields.

Like **1** [2] and **2** [4], the new complexes **3–6** are air-stable in the solid state but slowly decompose in aerobic solutions. They were characterised by elemental analyses and mass spectroscopy (Table 1). In the IR each shows five terminal CO absorptions in the region 2055–1910 cm^{-1} and a single absorption between 1785–1740 cm^{-1} assigned to the bridging carbonyl (Table 2). The symmetrical species display a singlet in their $^{31}P\{^1H\}$ NMR spectrum in the region typical of a coordinated phosphine or phosphite, while unsymmetrical **6** shows the expected two signals. At room temperature the seven carbonyls of **1–6** appear as a single resonance in the ^{13}C NMR spectra, attributable to two concomitant fluxional processes, namely trigonal rotation of iron tricarbonyl groups coupled with scrambling of carbonyls in the plane perpendicular to the diphosphine ligand [21].

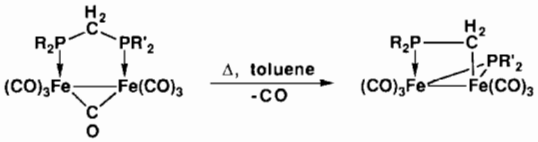

1	R = R' = Ph	7
2	R = R' = Me	8
3	R = R' = Et	9
4	R = R' = ^{i}Pr	10
5	R = R' = OEt	11
6	R = Ph, R' = Me	12

Synthesis of $[Fe_2(CO)_6(\mu\text{-}CH_2PR_2)(\mu\text{-}PR_2)]$ (7–12) via phosphorus–methylene bond cleavage

Heating toluene solutions of the complexes **1–5** results in a colour change from red to yellow, accompanied

TABLE 1. Physical, mass spectral and analytical data for new complexes

Complex	Colour	$M^{a,b}$	Analysis	
			C	H
3	red–orange	444(500)[c]	38.26(38.40)	4.45(4.40)
4	brown	528(556)[d]	44.60(43.17)	5.86(5.40)
5	red	564(564)	33.88(34.07)	4.13(3.93)
6	red	512(568)[c]	46.65(46.48)	3.41(3.17)
7	yellow	664(664)	56.60(56.02)	2.99(3.31)
8	yellow	416(416)	31.64(31.77)	3.48(3.39)
9	yellow	472(472)	37.94(38.13)	4.43(4.66)
10	yellow	500(528)[d]		
11	yellow	536(536)		
12	yellow	540(540)	47.06(46.67)	3.42(3.33)
14	yellow		53.64(54.44)	4.76(4.70)
15	yellow		61.73(61.33)	4.55(4.27)[e]
16	yellow		51.22(50.72)	4.68(4.59)[e]
17	red	678(706)[d]	55.82(56.13)	3.79(3.43)
18	yellow	538(538)	64.90(64.71)	4.38(4.49)
19	orange	600(600)	52.22(52.10)	3.00(3.00)
22	yellow	552(552)	65.93(65.22)	4.71(4.99)
23	orange	614(614)	52.41(52.77)	3.26(3.40)

[a]By mass spectrometry. [b]Calculated values in parentheses. [c]$(M\text{-}2CO)^+$. [d]$(M\text{-}CO)^+$. [e]Includes CH_2Cl_2 of crystallisation.

TABLE 2. IR and NMR data for new complexes

Complex	Carbonyl bands (cm^{-1})[a]	^{31}P NMR[b]	^{1}H NMR[b]	^{13}C NMR[b]
3	2041s, 1987s, 1971s, 1936s, 1916sh, 1744m	61.42(s)[c]	1.91 (m, 8H, CH_2Me), 1.79 (t, *J* 11, 2H, CH_2), 1.13 (quin, *J*8, 12H, Me)[c]	222.3 (t, *J* 7, CO), 26.1 (t, *J* 18, CH_2), 20.1 (t, *J* 17, CH_2Me), 6.9 (s, Me)
4	2039s, 1985s, 1970s, 1935s, 1915s, 1750m	82.75 (s)[c]	2.33 (m, 4H, $CHMe_2$), 1.85 (t, *J* 11, 2H, CH_2), 1.40 (dq, *J* 7, 2, 24 H, Me)[c]	22.9 (t, *J* 5, CO), 28.8 (t, *J* 13, CH_2), 20.0 (t, *J* 15, $CHMe_2$), 18.3 (s, Me)
5	2055s, 2003s, 1990s, 1964m, 1952s, 1784m, 1767m[d]	195.16(s)	3.95–3.80(m, 4H, CH_2Me), 3.70–3.56 (m, 4H, CH_2Me), 2.37 (t, *J* 12, 2H, CH_2), 1.10 (t, *J* 7, 12H, Me)	212.2 (t, *J* 5, CO), 63.3 (t, *J* 3, CH_2Me), 44.8 (t, *J* 34, CH_2), 15.8 (t, *J* 2, Me)
6	2048s, 1991s, 1977s, 1941s, 1923sh, 1750m	62.42 (d, *J* 93), 48.75 (d, *J* 93)	8.06–7.49 (m, 10H, Ph), 2.88 (t, *J* 11, 2H, CH_2), 1.36 (d, *J* 10, 6H, Me)	221.8 (t, *J* 7, CO), 134.0–128.0 (m, Ph), 44.4 (t, *J* 20, CH_2), 16.9 (dd, *J* 31, 5, Me)
7	2046s, 2004s, 1991s, 1963s, 1952m[d]	181.10 (d, *J* 32), 21.27 (d, *J* 32)	8.23–6.70 (m, 20H, Ph), 0.70 (dt, *J* 21, 12, 1H, C*H*H), 0.61 (dd, *J* 12, 6, 1H, CH*H*)[c]	213.0 (br, CO), 141.2–127.5 (m, Ph), −19.5 (t, *J* 5, CH_2)[d]
8	2045s, 2003s, 1971s, 1964s, 1944m[d]	137.00 (d, *J* 39), −0.71 (d, *J* 39)	2.01 (d, *J* 8, 3H, Me), 1.89 (d, *J* 9, 3H, Me), 1.69 (d, *J* 10, 3H, Me), 1.24 (d, *J* 9, 3H, Me), −0.31 (m, H, CH_2)	213.3 (t, *J* 7, CO), 25.5 (d, *J* 4, Me), 20.6 (dd, *J* 18, 4, Me), 19.3 (dd, *J* 31, 7, Me), 14.4 (d, *J* 13, Me), −12.8 (t, *J* 4, CH_2)
9	2049s, 2008s, 1979s, 1964s, 1950m[d]	176.92 (d, *J* 34), 22.11 (d, *J* 34)[c]	2.60–1.71 (m, 8H, CH_2), 1.58–0.73 (m, 12H, Me), −0.13 (ddd, *J* 12, 7, 4, 1H, C*H*H), −0.47 (dt, *J* 18, 12, 1H, CH*H*)	213.1 (t, *J* 8, CO), 25.7 (d, *J* 3, Me), 23.6 (dd, *J* 22, 3, CH_2Me), 19.8 (dd, *J* 30, 4, CH_2Me), 15.6 (d, *J* 11, Me), 11.2 (d, *J* 26, CH_2Me), 10.9 (d, *J* 25, CH_2Me), 6.3 (d, *J* 3, Me), 4.6 (d, *J* 7, Me), −19.1 (t, *J* 4, CH_2)
10	2045s, 2004s, 1973s, 1960s, 1944m[d]	212.29 (d, *J* 24), 42.41 (d, *J* 24)	1.34–1.02 (m, 28H, ^{i}Pr), 0.11 (ddd, *J* 13, 6, 4, 1H, C*H*H), −0.09 (dt, *J* 17, 13, 1H, CH*H*)	
11	2063s, 2023s, 1998s, 1983m, 1972s, 1962m[d]	327.52 (d, *J* 44), 165.67 (d, *J* 44)	4.05–3.79 (m, 4H, CH_2Me), 3.58–3.36 (m, 4H, CH_2Me), 1.23 (t, *J* 7, 3H, Me), 1.17 (t, *J* 7, 3H, Me), 1.15 (t, *J* 7, 3H, Me), 1.03 (t, *J* 7, 3H, Me), 0.96 (dt, *J* 30, 7, 1H, C*H*H), 0.48 (ddd, *J* 21, 7, 6, 1H, CH*H*)[e]	213.0 (t, *J* 12, CO), 67.3 (d, *J* 12, CH_2Me), 66.3 (d, *J* 12, CH_2Me), 61.2 (d, *J* 8, CH_2Me), 58.8 (d, *J* 10, CH_2Me), 16.2 (s, Me), 16.1 (s, Me), 16.0 (s, Me), 15.8 (s, Me), −4.9 (t, *J* 7, CH_2)[e]
12	2048s, 2066s, 1978s 1962s, 1942m[d]	128.05 (d, *J* 44), 33.89 (d, *J* 44)	7.73–7.10 (m, 10H, Ph), 2.09 (d, *J* 10, 3H, Me), 1.69 (d, *J* 11, 3H, Me), 0.94 (dt, *J*21, 13, 1H, C*H*H), 0.28 (ddd, *J* 13, 7, 4, 1H, CH*H*)	213.3 (t, *J* 4, CO), 140.0–128.0 (m, Ph), 20.6 (d, *J* 24, Me), 16.8 (d, *J* 13, Me), −16.8 (d, *J* 4, CH_2)
14	1946m, 1896s, 1871s 1846m, 1680m			

(*continued*)

TABLE 2. (*continued*)

Complex	Carbonyl bands (cm^{-1})[a]	^{31}P NMR[b]	^{1}H NMR[b]	^{13}C NMR[b]
15a	1971m, 1940s, 1900m, 1888sh	176.31 (ddd, *J* 43, 30, 25, P^1), 65.81 (ddd, *J* 118, 97, 43, P^2), 61.33 (ddd, *J* 118, 31, 30, P^3), 22.83 (ddd, *J* 97, 31, 25, P^4)	7.84–6.32 (m, Ph), 3.47 9dt, *J* 14, 10, 1H, PC*H*HP), 1.96 (q, *J* 14, 1H, PCH*H*P), 0.48 (dt, *J* 20, 12, 2H, PCH_2)	225–217 (unres., CO), 145–120 (m, Ph), 30.8 (t, *J* 19, PCH_2P), −18.6 (t, *J* 12, PCH_2)
15b	1971m, 1940s, 1900m, 1888sh	204.08 (ddd, *J* 87, 53, −22, P^1), 53.28 (m, *J* 103, 87, 9, P^3), 52.33 (m, *J* 103, −56, 53, P^2), 28.34 (ddd, *J* −56, −22, 9, P^4)	7.84–6.32 (m, Ph), 4.68 (q, *J* 11, 1H, PC*H*HP), 2.92 (m, 1H, PCH*H*P), 0.22 (br, 2H, PCH_2)	225–217 (unres., CO), 145–120 (m, Ph), 27.6 (t, *J* 22, PCH_2P), −19.8 (t, *J* 8, PCH_2
16a	1974m, 1938s, 1910s, 1892w[d]	110.66 (dd, *J* 50, 40, P^1), 39.18–15.30 (m, P^2, P^3), −1.63 (dd, *J* 78, 46, P^4)[f]		
17	2045s, 1993s, 1977s, 1943s, 1921sh, 1742m	71.24(s)	7.61–7.10 (m, 20H, Ph), 3.55 (qt, *J* 14, 7, 1H, C*H*Me), 1.40 (dt, *J* 10, 7, 3H, Me)	208.8 (t, *J* 5, CO), 122.3–112.8 (m, Ph), 33.8 (t, *J* 15, *C*HMe), 17.6 (s, Me)
18	1985s, 1909s, 1900s	33.01(s)	7.50 (s, 20H, Ph), 4.62 (m, 1H, C*H*Me), 0.81 (m, 3H, Me)	220.5 (t, *J* 6, CO), 137.7–127.6 (m, Ph), 51.6 (t, *J* 22, *C*HMe), 16.2 (t, *J* 6, Me)
19	2054s, 2010s, 1989m, 1970m, 1948w	156.44 (d, *J* 110), 44.51 (d, *J* 110)[c]	7.98–6.18 (m, 14H, Ph), 4.21 (dquin, *J* 16, 7, 1H, C*H*Me), 1.11 (dt, *J* 17, 7, 3H, Me)[c]	210.7 (br, CO), 145.3 (d, *J* 20, C_{ipso}), 133.0–128.4 (m, Ph), 122.6 (d, *J* 9, FeC), 47.9 (dd, *J* 24, 11, CHMe), 16.5 (t, *J* 7, Me)[c]
22	1983s, 1906s, 1900s	53.81(s)[c]	7.82–7.21 (m, 20H, Ph), 1.42 (t, *J* 15, 6H, Me)[c]	221.2 (t, *J* 7, CO), 134.7–127.9 (m, Ph), 61.6 (t, *J* 21, CMe_2), 27.3 (t, *J* 4, Me)[c]
23	2058s, 2013s, 1998s, 1968w, 1956m[d]	175.84 (d, *J* 112), 53.61 (d, *J* 112)[c]	7.88–6.18 (m, 14H, Ph), 1.53 (t, *J* 15, 3H, Me), 1.26 (t, *J* 18, 3H, Me)[c]	

[a]In CH_2Cl_2. [b]In CD_2Cl_2. [c]In $CDCl_3$. [d]In hexane. [e]In C_6D_6. [f]In toluene-d^8.

in the IR by the disappearance of the bridging carbonyl absorption of the starting materials. Chromatography permits the isolation of the yellow crystalline complexes $[Fe_2(CO)_6(\mu\text{-}CH_2PR_2)(\mu\text{-}PR_2)]$ (**7–11**) in 30–90% yields. The cleavage of dppm occurs much more readily than that of the other diphosphines, completion being reached in the order: Ph (10 min) > Me ≈ Et ≈ ^{i}Pr (1–2 h) > OEt (6 h). The ease of the process for dppm is emphasised by the fact that the transformation of **1** to **7** is completed equally quickly in refluxing tetrahydrofuran (b.p. 64 °C, cf. 111 °C for toluene).

The complexes **7–12** are air-stable both in the solid-state and in solution and are readily characterised on the basis of analytical and spectroscopic data (Tables 1 and 2). Thus, all show molecular ions in their mass spectra and five terminal CO bands in the IR. In the $^{31}P\{^1H\}$ NMR spectra the complexes exhibit two doublets, one at low field characteristic of a phosphido or phosphito group bridging a metal–metal bond [22], and a second at higher field due to the μ-phosphidomethyl ligand. The phosphorus–phosphorus coupling constant of 24–44 Hz is indicative of a *cis* disposition of the μ-phosphido and μ-phosphidomethyl ligands, as shown. The new Fe–CH_2 bond is revealed in a high field signal (δ −4.9 to −19.5 ppm) in the ^{13}C NMR spectra, while in the ^1H NMR spectra the methylene protons are also shifted to high field with respect to the uncleaved complexes.

A large number of dinuclear phosphido-bridged complexes is known [23], the majority containing the diphenylphosphido moiety; μ-dialkylphosphido [24] ligands are less common and μ-phosphito ligands appear to be unknown prior to this work. Complexes of the μ-phosphidomethyl ligand are also rare [25–31], but while this work was in progress Wojcicki and coworkers independently synthesised **7** via the reaction of the bis(phosphido) dianion $[Fe_2(CO)_5(\mu\text{-}CO)(\mu\text{-}PPh_2)(\eta^1\text{-}PPh_2)]^{2-}$ with di-iodomethane [32]. Work in the same group has also resulted in the synthesis and crystallographic characterisation of the cyano derivative $[Fe_2(CO)_6\{\mu\text{-}CH(CN)PPh_2\}(\mu\text{-}PPh_2)]$, shown to contain a *cis* arrangement of the phosphido and phosphidomethyl ligands [33]. A small number of other dinuclear metal complexes is known in which a metal–metal bond is bridged by both phosphido and phosphidomethyl ligands [34–37].

The cleavage of the phosphorus–methylene bond of a diphosphine ligand to yield a phosphidomethyl complex had not previously been reported when this work began. However, there was evidence which implicated such a process. Thus, Braterman *et al.* [38] isolated diphenylmethylphosphine from the thermolysis of $[PtPh_2(\eta^2\text{-dppm})]$, while thermolysis of the dicobalt complex $[Co_2(CO)_4(\mu\text{-}CO)_2(\mu\text{-dppm})]$ in the presence of hydrogen was reported [39] to produce the μ-phosphido compound $[Co_2(CO)_4(\mu\text{-}H)(\mu\text{-}PPh_2)(\mu\text{-dppm})]$. The fate of both fragments of a cleaved diphosphine was established in the rearrangement of $^iPr_2PCH_2PH^iPr$ at a tri-iron centre to give coordinated P^iPr_2Me and μ_3-P^iPr [40]. More recently, Riera *et al.* [41] have observed that thermolysis of the dimolybdenum complex $[Mo_2(CO)_4(\mu\text{-dppm})(\eta\text{-}C_5H_5)_2]$ results in phosphorus–methylene bond cleavage to produce $[Mo_2(CO)_2(\mu\text{-}CH_2PPh_2)(\mu\text{-}PPh_2)(\eta\text{-}C_5H_5)_2]$, in a process analogous to that described here. Another example of phosphorus–methylene bond cleavage in bis(dimethylphosphino)methane has recently been reported [42].

The cleaved products **7–11** arise from their precursors **1–5** by a combination of CO loss and apparent oxidative-addition of a P–CH_2 bond of the diphosphine. In Scheme 1 two likely pathways are shown, involving either initial CO loss or metal–metal bond cleavage to create the 16-electron iron centre required for oxidative-addition; the terminal phosphido ligand so-formed subsequently adopts a more favourable bridging site. Loss of CO does not appear to be the rate-determining step in the transformation since complexes **1** and **5**, which have the highest frequency CO stretching absorptions (Table 2), react fastest and slowest, respectively. Moreover, oxidative-addition might be expected to occur most readily for the better electron-donating alkylphosphines. It is clear that phenyl has a unique ability to promote P–CH_2 bond cleavage in this system, confirmed when reactions designed to provide competitive cleavage situations were investigated.

The complex $[Fe_2(CO)_6(\mu\text{-}CO)(Ph_2PCH_2PMe_2)]$ (**6**), readily prepared as described above, contains inequivalent P–CH_2 bonds and cleavage can thus, in principle, occur to give either $[Fe_2(CO)_6(\mu\text{-}CH_2PPh_2)(\mu\text{-}PMe_2)]$ or $[Fe_2(CO)_6(\mu\text{-}CH_2PMe_2)(\mu\text{-}PPh_2)]$. In fact, heating a toluene solution of **6** for 30 min led to exclusive and clean Me_2P–CH_2 bond cleavage, giving $[Fe_2(CO)_6(\mu\text{-}CH_2PPh_2)(\mu\text{-}PMe_2)]$ (**12**) in 84% yield. Characterisation was straightforward, being based on a comparison of the $^{31}P\{^1H\}$ NMR spectrum with those of **7** and **8**. Thus, two doublets were observed at δ 33.9 and 128.1 (J(PP) 44 Hz) ppm, the former typical of μ-CH_2PPh_2 (cf δ 21.3 ppm for **7**) and the latter of μ-PMe_2 (cf δ 137.0 ppm for **8**).

At first sight, the specific cleavage of the Me_2P–CH_2 bond of $Ph_2PCH_2PMe_2$ is at variance with the observation that dppm cleaves much faster than $Me_2PCH_2PMe_2$. However, the common factor is that the product containing the μ-CH_2PPh_2 ligand is favoured, suggesting that the direction of $Ph_2PCH_2PMe_2$ cleavage is controlled by the ability of the phenyl group to stabilise the CH_2PR_2 species. Further evidence of this was obtained when P–CH_2 cleavage in $[Fe_2(CO)_4(\mu\text{-}CO)(\mu\text{-}R_2PCH_2PR_2)_2]$ complexes was investigated, as described below.

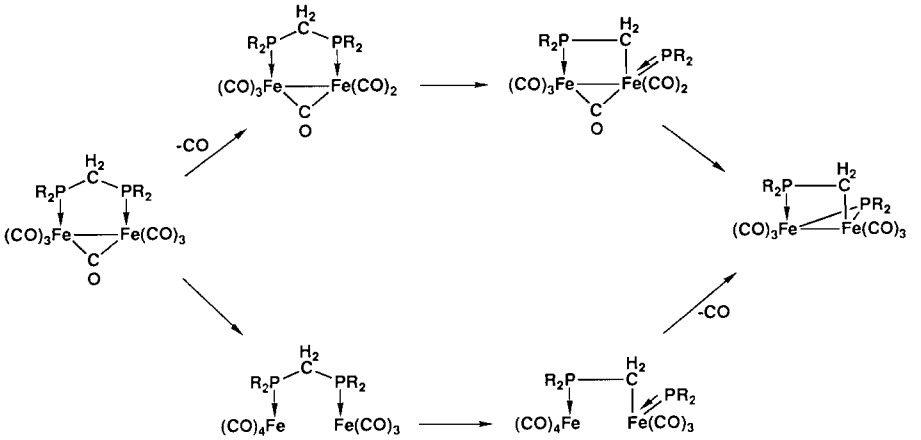

Scheme 1. Possible reaction pathways for P–CH_2 bond cleavage in diphosphines.

Phosphorus–methylene bond cleavage of [$Fe_2(CO)_4(\mu$-CO)(μ-$R_2PCH_2PR_2$)$_2$] (13, 14)

There have been several reports of the synthesis of complexes [$Fe_2(CO)_4(\mu$-CO)(μ-$R_2PCH_2PR_2$)$_2$] via the UV irradiation of the heptacarbonyl [$Fe_2(CO)_6(\mu$-CO)(μ-$R_2PCH_2PR_2$)] in the presence of an excess of the diphosphine [4–6, 8, 43]. In this way we prepared [$Fe_2(CO)_4(\mu$-CO)(μ-dppm)$_2$] (**13**) [5] and the new complex [$Fe_2(CO)_4(\mu$-CO)(μ-dppm)(μ-$Me_2PCH_2PMe_2$)] (**14**), the latter in order to investigate competitive P–CH_2 cleavage. Due to the highly air-sensitive nature of these complexes, characterisation was achieved only on the basis of analytical and IR spectroscopic data (Table 2).

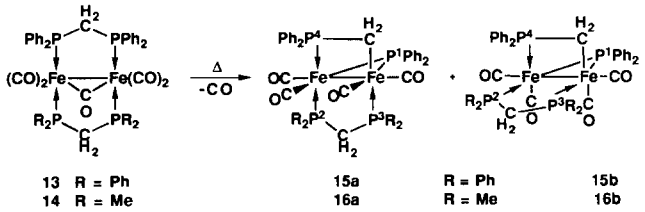

13 R = Ph
14 R = Me

15a R = Ph
16a R = Me

15b R = Ph
16b R = Me

Heating a toluene solution of **13** results in a gradual colour change from brown to orange over 16 h as the bridging carbonyl absorption disappears. Chromatography separates the cleaved product [$Fe_2(CO)_4(\mu$-CH_2PPh_2)(μ-PPh_2)(μ-dppm)] (**15**) in 95% yield as a mixture of two inseparable isomers **15a** and **15b** in *c.* 2:1 ratio. The existence of the isomers is clearly indicated by ^1H, ^{13}C and ^{31}P NMR data (Table 2), their assignment being based on the latter. Characterisation of the major isomer **15a** is staightforward since the $^{31}P\{^1H\}$ NMR spectrum is first order. The P–P couplings require a *cis* configuration for the phosphido (P^1) and phosphidomethyl (P^4) ligands ($J(P^1P^4)$ 25 Hz), with the former lying *cis* ($J(P^1P^2$ 43, $J(P^1P^3)$ 30 Hz) and the latter *trans* ($J(P^2P^4$ 97, $J(P^3P^4)$ 31 Hz) to the diphosphine (P^2, P^3). The structural assignment of the minor isomer **15b** is less straightforward because of the second order nature of its $^{31}P\{^1H\}$ NMR spectrum, but was achieved through computer simulation using the NUMARIT [44] program. The spectrum is again compatible with the phosphido and phosphidomethyl ligands being *cis* ($J(P^1P^4)$ −22 Hz), but requires that the dppm ligand is now *trans* to the phosphido ($J(P^1P^2)$ 53, $J(P^1P^3)$ 87 Hz) and *cis* to the phosphidomethyl ligand ($J(P^2P^4)$ −56, $J(P^3P^4)$ 9 Hz).

The 2:1 ratio of isomers revealed by ^1H NMR spectroscopy proved to be invariant with temperature up to 100 °C, indicating that the isomers are not in equilibrium.

The complex **14** was designed to provide another opportunity to compare the tendency towards Ph_2P–CH_2 and Me_2P–CH_2 bond cleavage. Heating **14** in toluene results in slow, specific cleavage of the dppm ligand over 10 days, the new complex [$Fe_2(CO)_4(\mu$-CH_2PPh_2)(μ-PPh_2)(μ-$Me_2PCH_2PMe_2$)] (**16**) being formed in 68% yield as the only product of the reaction. Like **15**, complex **16** exists as two isomers **16a** and **16b**, in the ratio of 10:1. Crystallisation from a dichloromethane–hexane solution led to the isolation of pure **16a**, the structure of which was established by X-ray diffraction, as described below. That both isomers arise from P–CH_2 bond cleavage in dppm is clearly shown by ^{31}P NMR spectroscopy, diphenylphosphido resonances being observed at δ 172.2 and 203.9 ppm for the major and minor isomers, respectively. ^{31}P NMR data confirm that in the major isomer **16a** the μ-$Me_2PCH_2PMe_2$ ligand lies *trans* to the phosphidomethyl and in the minor isomer **16b** *trans* to the phosphido, as shown. Complete assignment of the minor isomer **16b** proved difficult since the phosphidomethyl and diphosphine resonances are obscured by the more intense signals of **16a**.

The thermolyses of **13** and **14** confirm the generality of the phosphorus–methylene bond cleavage process at

the di-iron centre, but it is notable that the reaction is slowed significantly by the presence of a second diphosphine ligand. This strong σ-donor ligand results in the CO ligands being more strongly bound in **13** and **14** compared with their heptacarbonyl analogues (see IR data in Table 2), suggesting that in this system the loss of CO may be rate determining.

The Ph_2P–CH_2 bond cleavage observed for **14** and the Me_2P–CH_2 bond cleavage previously described for **6** are in apparent contradiction. Again, however, the cleavages fit the pattern that the μ-CH_2PPh_2 ligand is formed in preference to μ-CH_2PMe_2, consistent with a unique ability of the phenyl group to stabilise the phosphidomethyl ligand. A possible reason for this is discussed in the next section.

The possibility that the observed selectivity in P–CH_2 bond cleavage could be the result of thermodynamic control requires that the process be reversible. However, even under 250 atm pressure neither **12** nor **16** took up CO to reconstitute the corresponding diphosphine complex **6** or **14**; indeed, the complexes were unreactive under these conditions. The same proved to be the case for complex **7**.

Molecular structure of $[Fe_2(CO)_4(\mu\text{-}CH_2PPh_2)(\mu\text{-}PPh_2)(\mu\text{-}Me_2PCH_2PMe_2)]$ ***(16a)***

In order to confirm the nature of the selective bond cleavage process occurring upon thermolysis of **14**, and the structural assignments, an X-ray diffraction study was carried out on the major isomer **16a** as its dichloromethane solvate. The results are summarised in Fig. 1 and selected bond lengths and angles given in Table 3.

The structure is based on a singly bonded di-iron unit (Fe–Fe 2.699(1) Å) bridged symmetrically by $Me_2PCH_2PMe_2$ and diphenylphosphido ligands which

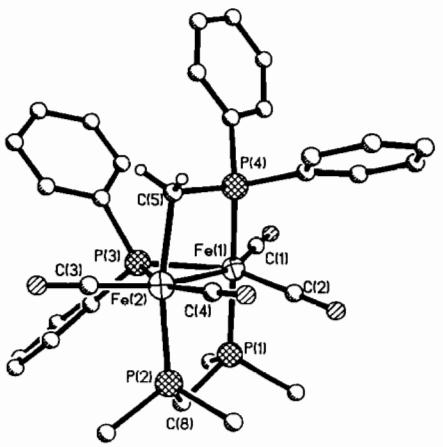

Fig. 1. Molecular structure of **16a**, showing atom labelling scheme. Phenyl and $Me_2PCH_2PMe_2$ group hydrogens have been omitted for clarity. Metal atoms are represented as ellipsoids enclosing 50% probability density, other atoms as spheres of arbitrary radii.

TABLE 3. Selected bond lengths and bond angles for **16a** · CH_2Cl_2

Bond lengths (Å)			
Fe(1)–Fe(2)	2.699(1)	Fe(1)–P(1)	2.229(2)
Fe(1)–P(3)	2.229(2)	Fe(1)–P(4)	2.255(2)
Fe(1)–C(1)	1.758(5)	Fe(1)–C(2)	1.768(5)
Fe(2)–P(2)	2.239(2)	Fe(2)–P(3)	2.218(2)
Fe(2)–C(3)	1.734(6)	Fe(2)–C(4)	1.766(5)
Fe(2)–C(5)	2.100(5)	P(1)–C(6)	1.822(6)
P(1)–C(7)	1.815(4)	P(1)–C(8)	1.826(6)
P(2)–C(8)	1.829(5)	P(2)–C(9)	1.825(6)
P(2)–C(10)	1.817(6)	P(3)–C(11)	1.843(4)
P(3)–C(21)	1.841(5)	P(4)–C(5)	1.787(6)
P(4)–C(31)	1.838(5)	P(4)–C(41)	1.842(5)
C(1)–O(1)	1.155(7)	C(2)–O(2)	1.161(6)
C(3)–O(3)	1.162(8)	C(4)–O(4)	1.152(6)
Bond angles (°)			
Fe(2)–Fe(1)–P(1)	97.5(1)	Fe(2)–Fe(1)–P(3)	52.5(1)
P(1)–Fe(1)–P(3)	92.0(1)	Fe(2)–Fe(1)–P(4)	72.4(1)
P(1)–Fe(1)–P(4)	168.5(1)	P(3)–Fe(1)–P(4)	86.3(1)
Fe(2)–Fe(1)–C(1)	160.8(2)	P(1)–Fe(1)–C(1)	90.3(2)
P(3)–Fe(1)–C(1)	110.0(2)	P(4)–Fe(1)–C(1)	101.0(2)
Fe(2)–Fe(1)–C(2)	88.2(2)	P(1)–Fe(1)–C(2)	86.1(2)
P(3)–Fe(1)–C(2)	140.1(2)	P(4)–Fe(1)–C(2)	87.9(2)
C(1)–Fe(1)–C(2)	109.9(2)	Fe(1)–Fe(2)–P(2)	89.7(1)
Fe(1)–Fe(2)–P(3)	52.8(1)	P(2)–Fe(2)–P(3)	97.5(1)
Fe(1)–Fe(2)–C(3)	153.4(2)	P(2)–Fe(2)–C(3)	97.0(2)
P(3)–Fe(2)–C(3)	100.6(2)	Fe(1)–Fe(2)–C(4)	104.9(2)
P(2)–Fe(2)–C(4)	89.0(2)	P(3)–Fe(2)–C(4)	156.5(2)
C(3)–Fe(2)–C(4)	101.0(3)	Fe(1)–Fe(2)–C(5)	82.4(2)
P(2)–Fe(2)–C(5)	168.9(2)	P(3)–Fe(2)–C(5)	84.1(1)
C(3)–Fe(2)–C(5)	93.5(2)	C(4)–Fe(2)–C(5)	85.5(2)
Fe(1)–P(1)–C(6)	115.9(2)	Fe(1)–P(1)–C(7)	119.3(2)
C(6)–P(1)–C(7)	99.6(3)	Fe(1)–P(1)–C(8)	113.5(2)
C(6)–P(1)–C(8)	103.0(3)	C(7)–P(1)–C(8)	103.3(2)
Fe(2)–P(2)–C(8)	116.4(2)	Fe(2)–P(2)–C(9)	114.6(2)
C(8)–P(2)–C(9)	102.2(2)	Fe(2)–P(2)–C(10)	119.0(2)
C(8)–P(2)–C(10)	102.5(2)	C(9)–P(2)–C(10)	99.4(3)
Fe(1)–P(3)–Fe(2)	74.7(1)	Fe(1)–P(3)–C(11)	126.0(2)
Fe(2)–P(3)–C(11)	124.1(2)	Fe(1)–P(3)–C(21)	122.1(2)
Fe(2)–P(3)–C(21)	120.0(1)	C(11)–P(3)–C(21)	93.2(2)
Fe(1)–P(4)–C(5)	103.8(2)	Fe(1)–P(4)–C(31)	114.0(2)
C(5)–P(4)–C(31)	108.7(2)	Fe(1)–P(4)–C(41)	123.2(2)
C(5)–P(4)–C(41)	109.8(2)	C(31)–P(4)–C(41)	96.9(2)
Fe(1)–C(1)–O(1)	177.9(4)	Fe(1)–C(2)–O(2)	178.5(5)
Fe(2)–C(3)–O(3)	179.3(5)	Fe(2)–C(4)–O(4)	177.2(5)
Fe(2)–C(5)–P(4)	98.3(2)	Fe(2)–C(5)–H(5a)	115.6(23)
P(4)–C(5)–H(5a)	110.0(26)	Fe(2)–C(5)–H(5b)	113.1(31)
P(4)–C(5)–H(5b)	112.9(32)	H(5a)–C(5)–H(5b)	107.0(38)
P(1)–C(8)–P(2)	111.6(2)		

form planes with the iron–iron bond at slightly more than right angles to one another (P(2)–Fe(2)–P(3) 97.5(1)°, P(1)–Fe(1)–P(3) 92.0(1)°). The metal–metal bond is also bridged by a CH_2PPh_2 ligand which lies *trans* to the diphosphine and *cis* to the phosphido so that the P(3)–Fe(1)–P(4) bond angle is 86.3(1)°. The four-membered ring containing the phosphidomethyl ligand and the di-iron unit is slightly puckered, with a torsion angle around the P(4)–C(5) bond of 16.2(2)°, while the Ph_2P–CH_2 bond length is indicative of a bond

order greater than unity (1.787(6) Å cf. other P(4)–C of 1.838(5) and 1.842(5) Å). Each iron atom also carries two terminal carbonyl groups, one *trans* to the phosphido bridge and the other *trans* to the metal–metal bond, so that the coordination geometry around each iron can be described as a distorted octahedron. The average Fe–CO bond length is only 1.76 Å, compared with an average of 1.80 Å for the hexacarbonyl complex $[Fe_2(CO)_6\{\mu\text{-}CH(CN)PPh_2\}(\mu\text{-}PPh_2)]$ [33], reflecting the strong π-backdonation induced by the presence of the $Me_2PCH_2PMe_2$ ligand. Compared with $[Fe_2(CO)_6\{\mu\text{-}CH(CN)PPh_2\}(\mu\text{-}PPh_2)]$ there is also a significantly shorter Fe–Fe bond in **16a** (2.699 versus 2.807 Å).

Klein *et al.* [45] have suggested that the bonding of a μ-phosphidomethyl ligand can be represented by three resonance forms **A**, **B** and **C**, as shown below, and it is clear from the P–CH_2 bond length in **16a** that **C** makes a significant contribution. Other structural studies on μ-phosphidomethyl complexes have shown a similar effect; indeed, such species are sometimes referred to as ylide complexes. However, the zwitterionic form **B** may offer a clue to understanding the observation that phenyl groups strongly stabilise the phosphidomethyl ligand, in that they will be able to disperse the positive charge on phosphorus into their ring system. A further consequence of this form being significant is that the presence of electron-donating groups on the carbon should lower the stability of **B** and therefore tend to suppress the P–CH_2 bond cleavage process. With this in mind, the effect of methyl substitution on the CH_2 carbon of dppm was investigated.

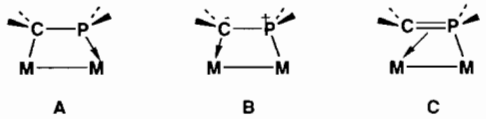

Effect of methyl substitution in $Ph_2CH_2PPh_2$ on P–C bond cleavage

While complexes containing the diphosphines $R_2PCH_2PR_2$ are common, derivatives containing modifications at the backbone carbon remain rare [10]. However, treatment of 1,1-bis(diphenylphosphino)-ethane, $Ph_2PCH(Me)PPh_2$, with $[Fe_2(CO)_9]$ and $[Fe(CO)_5]$ readily affords $[Fe_2(CO)_6(\mu\text{-}CO)\{\mu\text{-}Ph_2PCH(Me)PPh_2\}]$ (**17**) in 95% yield. Heating a toluene solution of **17** for 5 min, followed by chromatography led to the isolation of two products. The major product, yellow mononuclear $[Fe(CO)_3\{\eta^2\text{-}Ph_2PCH(Me)PPh_2\}]$ (**18**), was formed in 32% yield as a result of metal–metal bond cleavage and is analogous to $[Fe(CO)_3(\eta^2\text{-dppm})]$ [19]. The other, more interesting product was orange $[Fe_2(CO)_6\{\mu\text{-}PhPCH(Me)PPh(C_6H_4\text{-}o)\}]$ (**19**), isolated in 19% yield. Prior to chromatography, a $^{31}P\{^1H\}$ NMR spectrum of the crude reaction mixture revealed the presence of two doublets at δ 178.1 and 23.6 (J(PP) 32 Hz) ppm, similar to those of complex **7** and consistent with the formation of the P–CHMe bond-cleavage product $[Fe_2(CO)_6\{\mu\text{-}CH(Me)PPh_2\}(\mu\text{-}PPh_2)]$ (**20**), but this was present in less than 1% yield and did not survive chromatography.

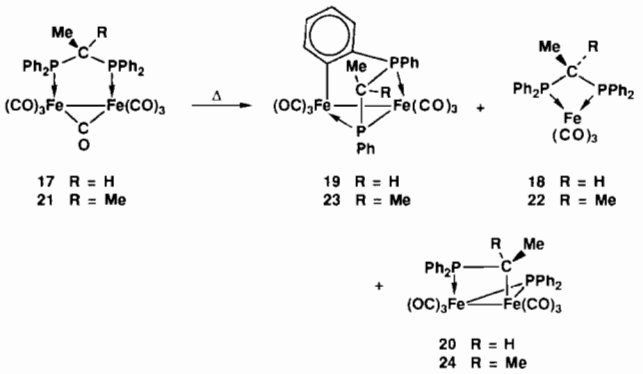

Complex **19** is formed as a result of benzene and carbon monoxide loss from **17**, clearly shown by the presence of a molecular ion in the mass spectrum. In the $^{31}P\{^1H\}$ NMR spectrum there were two doublets at δ 156.4 and 44.5 (J(PP) 110 Hz) ppm typical of phosphido and phosphine moieties, respectively, but an X-ray diffraction study was required in order to identify the complex.

Molecular structure of $[Fe_2(CO)_6\{\mu\text{-}PhPCH(Me)\text{-}PPh(C_6H_4\text{-}o)\}]$ (19)

The results of the X-ray diffraction study on **19** are summarised in Fig. 2 and selected bond lengths and angles are listed in Table 4. The molecule contains a single-bonded di-iron unit (Fe–Fe 2.755(2) Å), with each iron atom carrying three terminal carbonyls. The

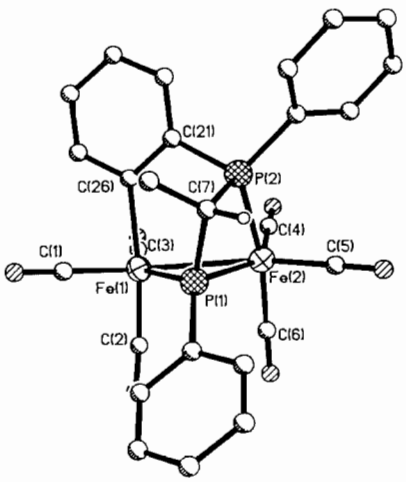

Fig. 2. Molecular structure of **19**, showing atom labelling scheme. Aryl and methyl group hydrogens have been omitted for clarity. Metal atoms are represented as ellipsoids enclosing 50% probability density, other atoms as spheres of arbitrary radii.

TABLE 4. Selected bond lengths and angles for **19**

Bond lengths (Å)			
Fe(1)–Fe(2)	2.755(2)	Fe(1)–P(1)	2.180(2)
Fe(1)–C(1)	1.775(6)	Fe(1)–C(2)	1.807(5)
Fe(1)–C(3)	1.801(6)	Fe(1)–C(26)	2.075(5)
Fe(2)–P(1)	2.206(2)	Fe(2)–P(2)	2.244(2)
Fe(2)–C(4)	1.792(5)	Fe(2)–C(5)	1.775(5)
Fe(2)–C(6)	1.787(5)	P(1)–P(2)	2.580(2)
P(1)–C(7)	1.844(5)	P(1)–C(11)	1.826(6)
P(2)–C(7)	1.850(5)	P(2)–C(21)	1.805(5)
P(2)–C(31)	1.819(5)	C(1)–O(1)	1.146(7)
C(2)–O(2)	1.135(6)	C(3)–O(3)	1.148(7)
C(4)–O(4)	1.144(6)	C(5)–O(5)	1.148(6)
C(6)–O(6)	1.147(6)	C(7)–H(7)	0.978(35)
C(7)–C(8)	1.512(7)		
Bond angles (°)			
Fe(2)–Fe(1)–P(1)	51.5(1)	Fe(2)–Fe(1)–C(1)	150.2(2)
P(1)–Fe(1)–C(1)	99.6(2)	Fe(2)–Fe(1)–C(2)	95.4(2)
P(1)–Fe(1)–C(2)	92.7(2)	C(1)–Fe(1)–C(2)	93.2(2)
Fe(2)–Fe(1)–C(3)	95,7(2)	P(1)–Fe(1)–C(3)	147.2(2)
C(1)–Fe(1)–C(3)	112.3(2)	C(2)–Fe(1)–C(3)	93.1(2)
Fe(2)–Fe(1)–C(26)	91.7(1)	P(1)–Fe(1)–C(26)	97.7(1)
C(1)–Fe(1)–C(26)	84.4(2)	C(2)–Fe(1)–C(26)	169.6(2)
C(3)–Fe(1)–C(26)	78.6(2)	Fe(1)–Fe(2)–P(1)	50.7(1)
Fe(1)–Fe(2)–P(2)	81.9(1)	P(1)–Fe(2)–P(2)	70.9(1)
Fe(1)–Fe(2)–C(4)	95.3(2)	P(1)–Fe(2)–C(4)	143.7(2)
P(2)–Fe(2)–C(4)	95.0(2)	Fe(1)–Fe(2)–C(5)	154.1(2)
P(1)–Fe(2)–C(5)	103.5(2)	P(2)–Fe(2)–C(5)	92.0(2)
C(4)–Fe(2)–C(5)	110.4(2)	Fe(1)–Fe(2)–C(6)	88.9(2)
P(1)–Fe(2)–C(6)	97.8(2)	P(2)–Fe(2)–C(6)	168.3(2)
C(4)–Fe(2)–C(6)	92.8(2)	C(5)–Fe(2)–C(6)	93.3(2)
Fe(1)–P(1)–Fe(2)	77.8(1)	Fe(1)–P(1)–P(2)	87.3(1)
Fe(2)–P(1)–P(2)	55.3(1)	Fe(1)–P(1)–C(7)	115.6(2)
Fe(2)–P(1)–C(7)	97.2(2)	P(2)–P(1)–C(7)	45.8(2)
Fe(1)–P(1)–C(11)	125.2(2)	Fe(2)–P(1)–C(11)	128.1(2)
P(2)–P(1)–C(11)	147.3(2)	C(7)–P(1)–C(11)	108.1(2)
Fe(2)–P(2)–P(1)	53.9(1)	Fe(2)–P(2)–C(7)	95.7(2)
P(1)–P(2)–C(7)	45.6(1)	Fe(2)–P(2)–C(21)	113.5(1)
P(1)–P(2)–C(21)	101.6(2)	C(7)–P(2)–C(21)	102.9(2)
Fe(2)–P(2)–C(31)	123.5(2)	P(1)–P(2)–C(31)	146.0(2)
C(7)–P(2)–C(31)	110.4(2)	C(21)–P(2)–C(31)	108.3(2)
Fe(1)–C(1)–O(1)	175.1(4)	Fe(1)–C(2)–O(2)	174.9(5)
Fe(1)–C(3)–O(3)	177.8(4)	Fe(2)–C(4)–O(4)	179.5(4)
Fe(2)–C(5)–O(5)	176.3(5)	Fe(2)–C(6)–O(6)	178.5(5)
P(1)–C(7)–P(2)	88.6(2)	P(1)–C(7)–H(7)	106.7(22)
P(2)–C(7)–H(7)	108.8(24)	P(1)–C(7)–C(8)	119.0(4)
P(2)–C(7)–C(8)	122.8(4)	H(7)–C(7)–C(8)	108.8(21)

complex phosphine–phosphido ligand formed via benzene loss from $Ph_2PCH(Me)PPh_2$ chelates Fe(2) while bridging the Fe(1)–Fe(2) bond. The phosphido phosphorus P(1) bridges the di-iron centre slightly asymmetrically, as shown by the Fe(1)–P(1) and Fe(2)–P(1) bond lengths of 2.180(2) and 2.206(2) Å, respectively. The two phosphorus atoms are linked symmetrically by the backbone carbon atom C(7) (P(1)–C(7) 1.844(5), P(2)–C(7) 1.850(5) Å) and each also carries a phenyl group. A second phenyl ring on phosphine atom P(2) is *ortho*-metalated by Fe(1), creating the five-membered ring Fe(2)–P(2)–C(21)–C(26). The four-membered chelate ring Fe(2)–P(2)–C(7)–P(1) is puckered (intra-ring torsion angles *c.* ±21°) so as to relieve non-bonded contacts involving the methylene substituent C(8). Ring closure constraints lead to a remarkably small P(1)–C(7)–P(2) angle of 88.6(2)° and a very short transannular P···P distance of 2.580(2) Å, only *c.* 0.3 Å longer than expected for a P–P single bond. A direct phosphorus–phosphorus bonding interaction is, however, usually indicated by a coupling constant *J*(PP) *c.* 500 Hz rather than the 110 Hz observed for **19**.

The 'parent' unsubstituted version of the bridging ligand in **19** has also been observed in the di- and triruthenium complexes $[Ru_2(CO)_6\{\mu\text{-}PhPCH_2PPh(C_6H_4\text{-}o)\}]$ and $[Ru_3(CO)_9\{\mu\text{-}\eta^3\text{-}PhPCH_2PPh(C_6H_4\text{-}o)\}]$ [46]. In the former complex a similar short P···P contact is observed (2.615 Å), accompanied by a moderate *J*(PP) 71 Hz. Interestingly, very little distortion of the *ortho*-metalated ring is observed in these complexes, the P–C_{ipso} bond length being only marginally shorter for this ring compared with the phenyl groups (e.g. for **19**: P(2)–C(21) 1.805(5), P(1)–C(11) 1.826(6), P(2)–C(31) 1.819(5) Å).

The structure of **19** is remarkably similar to that expected for P–CHMe bond cleavage, i.e. **20**, in that each is based on an $Fe_2(CO)_6$ unit bridged by a μ-phosphido and contains a terminal phosphine which is linked to the other iron through a σ-bound carbon, albeit in **19** as part of a five-membered ring. It is clear, therefore, that although methyl substitution suppresses P–CHMe bond cleavage in complex **17** the molecule finds other cleavage pathways to produce a product of the same stable structural type.

It seems likely that the formation of complex **19** is induced by loss of carbon monoxide, followed by oxidative-addition of an *ortho*-C–H bond of a phenyl ring, i.e. *ortho*-metalation. This will generate a metal hydride ligand, to be lost as benzene after oxidative-addition of a P–Ph bond of the other phosphorus. Phosphorus–phenyl bond cleavage reactions of dppm have been reported for a number of dimetal centres and in one example the cleaved phenyl group was found σ-bound to the metal [47]. Precedent exists for the *ortho*-metalation of μ-dppm at a dimetal centre [48, 49] but, unlike here, the *ortho*-carbon is invariably found bound to the same metal atom as the phosphorus atom. *Ortho*-metalation with the distant metal atom has been observed for bridging 1,2-bis(diphenylphosphino)ethane [50].

Substitution of two methyl groups on the linking carbon of dppm backbone favours the *ortho*-metalation pathway more strongly still. Thus, reaction of 2,2-bis(diphenylphosphino)propane with iron carbonyls results not in the formation of the expected heptacarbonyl complex $[Fe_2(CO)_6(\mu\text{-}CO)\{\mu\text{-}Ph_2PC(Me_2)PPh_2\}]$ (**21**), but mononuclear $[Fe(CO)_3\{\eta^2\text{-}Ph_2PC(Me_2)PPh_2\}]$ (**22**),

in 85% yield. An effort to convert the latter to **21**, via UV irradiation in the presence of an excess of iron pentacarbonyl, gave $[Fe_2(CO)_6\{\mu\text{-}PhPC(Me_2)PPh(C_6H_4\text{-}o)\}]$ (**23**) directly in 49% yield. Monitoring of the reaction by IR spectroscopy provided no evidence for the formation of **21** or **24**, indicating that this species must undergo very ready *ortho*-metalation at room temperature.

It is clear that methyl substitution on the linking carbon of μ-dppm suppresses the P–CH_2 cleavage process and promotes instead an *ortho*-metalation pathway, i.e. oxidative-addition of an *ortho* C–H bond of a phenyl group occurs in preference to a P–C bond. A study of the reaction of the diphosphines $Ph_2PC(RR')PPh_2$ ($RR' = H_2$, HMe or Me_2) with $[MnMe(CO)_5]$ led to the suggestion that the ratio of the *fac* and *mer* isomers of the products $[Mn(COMe)(CO)_3\{\eta^2\text{-}Ph_2PC(RR')PPh_2\}]$ was determined by steric interactions between the phenyl rings and the acyl ligand, which increase upon methyl substitution due to strong intra-phosphine methyl–phenyl interactions [51]. The possibility that a similar steric effect was operating in our system, the methyl group(s) forcing a phenyl group to adopt a position so that an *ortho* hydrogen is brought closer to iron, in place for *ortho*-metalation, led us to attempt the X-ray structure analysis of **17** as its hexane solvate, for comparison with that reported for unsubstituted **1** [2]. However only a poor refinement of the structure was possible (*R* 13.6), associated with low diffraction quality. However, the gross structural features of **17** are almost identical to those found for **1** [2]. The most evident difference between the two structures is the orientation of the phenyl rings, leading to the tentative suggestion that the methyl group (which lies in the pseudo-equatorial site on the central carbon atom of the substituted dppm ligand) may exert some steric control over the solid-state orientations of the phenyl rings. However, the two complexes crystallise in different space groups and intermolecular forces may account for this structural change. The structural study does not therefore provide strong evidence of a steric effect being responsible for the different bond cleavage processes undergone by **1** and **17** or **21**.

Earlier, we noted that there was a strong driving force for the production of the μ-CH_2PPh_2 ligand when diphosphines undergo P–CH_2 bond cleavage and attributed this to the ability of phenyl to stabilise positive charge on phosphorus in the resonance from **B**. In this same form the negative charge resides on the carbon of the μ-CH_2PPh_2 ligand and, clearly, methyl substitution at this carbon will destabilise the species through intensification of the charge. The suppression of the P–CH_2 bond cleavage process upon methyl substitution may therefore be traceable to this electronic effect.

Experimental

All reactions were carried out under a nitrogen atmosphere using dried and degassed solvents. Separation of products was achieved by column chromatography on alumina. Photolysis reactions were carried out in silica glass tubes, using a 500 W mercury vapour lamp as the source of UV radiation. Elemental analyses were performed by the Microanalytical Laboratory of the School of Chemistry. IR spectra were recorded on a Nicolet 5-MX Fourier Transform spectrometer using calcium fluoride cells of 1 mm path length. Low resolution electron impact mass spectra were recorded using an AEI MS 902 instrument operating at 70 eV. Proton and ^{13}C NMR spectra were recorded on JEOL FX 90, FX 200, GX 270 and GX 400 spectrometers, and ^{31}P NMR spectra on JEOL FX 90 and GX 400 instruments. Bis(diphenylphosphino)methane, 1,1-bis(diphenylphosphino)ethane, 2,2-bis(diphenylphosphino)propane and (dimethylphosphino)(diphenylphosphino)methane were prepared by literature methods [52, 53]. Bis(diethylphosphino)methane, bis(diisopropylphosphino)methane, and bis(diethoxyphosphino)methane were prepared by Dr B. R. Lloyd following literature methods [54, 55].

Synthesis of $[Fe_2(CO)_6(\mu\text{-}CO)(\mu\text{-diphosphine})]$ complexes

$[Fe_2(CO)_6(\mu\text{-}CO)(\mu\text{-dppm})]$ (**1**). A thf solution (150 cm^3) of $[Fe_2(CO)_9]$ (5.00 g, 13.73 mmol) and dppm (3.0 g, 7.81 mmol) was stirred for 3 h at room temperature, becoming red. It was then transferred to a silica glass tube and $[Fe(CO)_5]$ (1.0 cm^3, 7.60 mmol) added. UV irradiation for 16 h produced a dark red solution from which unreacted iron carbonyl and solvent were removed at reduced pressure. Chromatography, eluting with dichloromethane–hexane (2:3), yielded a red band from which 5.14 g (95%) of red crystalline $[Fe_2(CO)_6(\mu\text{-}CO)(\mu\text{-dppm})]$ (**1**) was obtained. Recrystallisation at −20 °C from dichloromethane–hexane solution afforded large dark red crystals.

Other complexes were synthesised in a similar manner. Thus, $Me_2PCH_2PMe_2$ afforded orange crystalline $[Fe_2(CO)_6(\mu\text{-}CO)(\mu\text{-}Me_2PCH_2PMe_2)]$ (**2**) (70%); $Et_2PCH_2PEt_2$, red–orange crystalline $[Fe_2(CO)_6(\mu\text{-}CO)(\mu\text{-}Et_2PCH_2PEt_2)]$ (**3**) (90%); $^iPr_2PCH_2P^iPr_2$, red–brown $[Fe_2(CO)_6(\mu\text{-}CO)(\mu\text{-}^iPr_2PCH_2P^iPr_2)]$ (**4**) (27%); $(EtO)_2PCH_2P(OEt)_2$, red $[Fe_2(CO)_6(\mu\text{-}CO)\{\mu\text{-}(EtO)_2PCH_2P(OEt)_2\}]$ (**5**) (45%); $Ph_2PCH_2PMe_2$, red $[Fe_2(CO)_6(\mu\text{-}CO)(\mu\text{-}Ph_2PCH_2PMe_2)]$ (**6**) (15%); $Ph_2PCH(Me)PPh_2$, red $[Fe_2(CO)_6(\mu\text{-}CO)\{\mu\text{-}Ph_2PCH(Me)PPh_2\}]$ (**17**) (95%).

Synthesis of $[Fe_2(CO)_6(\mu\text{-}CH_2PR_2)(\mu\text{-}PR_2)]$ complexes

$[Fe_2(CO)_6(\mu\text{-}CH_2PPh_2)(\mu\text{-}PPh_2)]$ (**7**). A toluene solution (100 cm^3) of **1** (0.20 g, 0.29 mmol) was refluxed for 10 min, resulting in a colour change from red to yellow. Chromatography, eluting with dichloromethane–hexane (1:4), gave a yellow band which afforded $[Fe_2(CO)_6(\mu\text{-}CH_2PPh_2)(\mu\text{-}PPh_2)]$ (**7**) (0.17 g, 90%) as a yellow microcrystalline solid. Recrystallisation from a cooled hexane solution afforded large yellow crystals.

Other complexes were synthesised in a similar manner. Thus, heating **2** (0.20 g, 0.45 mmol) for 2 h gave yellow $[Fe_2(CO)_6(\mu\text{-}CH_2PMe_2)(\mu\text{-}PMe_2)]$ (**8**) (0.12 g, 64%); **3** (0.30 g, 0.60 mmol) for 2 h yellow $[Fe_2(CO)_6(\mu\text{-}CH_2PEt_2)(\mu\text{-}PEt_2)]$ (**9**) (0.25 g, 90%); **4** (0.10 g, 0.18 mmol) for 30 min oily yellow $[Fe_2(CO)_6(\mu\text{-}CH_2P^iPr_2)(\mu\text{-}P^iPr_2)]$ (**10**) (0.03 g, 32%); **5**, (0.04 g, 0.07 mmol) for 6 h oily yellow $[Fe_2(CO)_6\{\mu\text{-}CH_2P(OEt)_2\}\{\mu\text{-}P(OEt)_2\}]$ (**11**) (0.03 g, 68%); **6** (0.09 g, 0.17 mmol) for 30 min yellow $[Fe_2(CO)_6(\mu\text{-}CH_2PPh_2)(\mu\text{-}PMe_2)]$ (**12**) (0.08 g, 84%).

Synthesis of $[Fe_2(CO)_4(\mu\text{-}CO)(\mu\text{-}dppm)(\mu\text{-}R_2PCH_2PR_2)]$ complexes

A toluene solution (150 cm^3) of **1** (0.50 g, 0.72 mmol) and dppm (0.31 g, 0.85 mmol) was subjected to UV irradiation for 5 h while purging with nitrogen, changing colour from red to brown. Removal of solvent left an oily brown solid which was washed with 3×20 cm^3 portions of hexane to yield $[Fe_2(CO)_4(\mu\text{-}CO)(\mu\text{-}dppm)_2]$ (**13**) (0.42 g, 57%) as a brown microcrystalline solid.

Similar irradiation of **1** (0.50 g, 1.13 mmol) with $Me_2PCH_2PMe_2$ (0.47 g, 1.24 mmol) afforded $[Fe_2(CO)_4(\mu\text{-}CO)(\mu\text{-}dppm)(\mu\text{-}Me_2PCH_2PMe_2)]$ (**14**) (0.52 g, 60%) as a yellow–orange powder.

Synthesis of $[Fe_2(CO)_4(\mu\text{-}CH_2PPh_2)(\mu\text{-}PPh_2)(\mu\text{-}R_2PCH_2PR_2)]$ complexes

A toluene solution (150 cm^3) of **13** (0.15 g, 0.15 mmol) was refluxed for 16 h, resulting in a colour change from brown to orange. Chromatography, eluting with dichloromethane–hexane (3:7), gave a yellow band which afforded $[Fe_2(CO)_4(\mu\text{-}CH_2PPh_2)(\mu\text{-}PPh_2)(\mu\text{-}dppm)]$ (**15**) (0.14 g, 96%) as a yellow powder. Yellow crystals were grown from a cooled dichloromethane–hexane solution.

Similar thermolysis of **14** (0.60 g, 0.78 mmol) for 10 days afforded $[Fe_2(CO)_4(\mu\text{-}CH_2PPh_2)(\mu\text{-}PPh_2)(\mu\text{-}Me_2PCH_2PMe_2)]$ (**16**) (0.58 g, 68%) as a yellow crystalline solid. Recrystallisation from a cooled dichloromethane–hexane solution gave yellow crystals of **16a** suitable for X-ray crystallography.

Synthesis of $[Fe_2(CO)_6\{\mu\text{-}PhPCH(Me)P(Ph)(C_6H_4\text{-}o)\}]$ (19)

Refluxing a toluene solution (150 cm^3) of $[Fe_2(CO)_6(\mu\text{-}CO)\{\mu\text{-}Ph_2PCH(Me)PPh_2\}]$ (**7**) (0.40 g, 0.57 mmol) resulted in a colour change from red to brown. ^{31}P NMR spectroscopy revealed a mixture of four products, the two minor constituents of which, $[Fe(CO)_4\{\eta^1\text{-}Ph_2PCH(Me)PPh_2\}]$ and $[Fe_2(CO)_6\{\mu\text{-}CH(Me)PPh_2\}(\mu\text{-}PPh_2)]$ (**20**), were identified only on this basis. Chromatography, eluting with dichoromethane–hexane (1:4), gave a yellow band which afforded $[Fe_2(CO)_6\{\mu\text{-}PhPCH(Me)P(Ph)(C_6H_4\text{-}o)\}]$ (**19**) (0.08 g, 19%) as a yellow crystalline solid. A second yellow band, eluted with dichloromethane–hexane (1:1), afforded $[Fe(CO)_3\{\eta^2\text{-}Ph_2PCH(Me)PPh_2\}]$ (**18**) (0.12 g, 32%) as a yellow crystalline solid.

Synthesis of $[Fe(CO)_3\{\eta^2\text{-}Ph_2PC(Me_2)PPh_2\}]$ (22)

A thf solution (200 cm^3) of $[Fe_2(CO)_9]$ (1.90 g, 5.22 mmol) and $Ph_2PC(Me_2)PPh_2$ (1.10 g, 2.67 mmol) was stirred at room temperature for 3 h, becoming orange. Chromatography, eluting with dichloromethane–hexane (3:7), gave a yellow band which afforded $[Fe(CO)_3\{\eta^2\text{-}Ph_2PC(Me_2)PPh_2\}]$ (**22**) (1.24 g, 85%) as a yellow microcrystalline solid.

Synthesis of $[Fe_2(CO)_6\{\mu\text{-}PhPC(Me_2)P(Ph)(C_6H_4\text{-}o)\}]$ (23)

UV irradiation of a thf solution (100 cm^3) of **22** (0.10 g, 0.19 mmol) and $[Fe(CO)_5]$ (0.5 cm^3), 3.80 mmol) for 20 h whilst purging with nitrogen resulted in a colour change from yellow to brown. Chromatography, eluting with dichloromethane–hexane (3:7), gave a yellow band which afforded $[Fe_2(CO)_6\{\mu\text{-}PhPC(Me)_2P(Ph)(C_6H_4\text{-}o)\}]$ (**23**) (0.06 g, 49%) as an orange crystalline solid.

Attempted carbonylation reactions

Subjecting toluene solutions (30 cm^3) of **7** (0.10 g, 0.15 mmol), **12** (0.05 g, 0.09 mmol) and **16** (0.10 g, 0.13 mmol) to 250 atm of carbon monoxide for 18, 16 and 16 h, respectively, led to no change in the IR spectrum. Chromatography resulted only in the recovery of starting material in each case.

Crystallographic studies of $\mathbf{16a}\cdot CH_2Cl_2$, $\mathbf{17}\cdot C_6H_{14}$ and 19

Many of the details of the structure analyses carried out on $\mathbf{16a}\cdot CH_2Cl_2$ and **19** are listed in Table 5. All X-ray diffraction measurements were made using Nicolet four-circle P3m diffractometers on single crystals mounted in thin-walled glass capillaries at room temperature using graphite-monochromated Mo Kα X-radiation ($\bar{\lambda}$=0.71069 Å). Cell dimensions for each analysis were determined from the setting angle values

TABLE 5. Details of structure analyses

	16a·CH_2Cl_2	**19**
Crystal data		
Formula	$C_{35}H_{36}Cl_2Fe_2O_4P_4$	$C_{26}H_{18}Fe_2O_6P_2$
Molecular weight	827.15	600.1
Crystal system	monoclinic	monoclinic
Space group (No.)	$P2_1/n$ (No. 14)	$P2_1/c$ (No. 14)
a (Å)	21.655(7)	11.602(5)
b (Å)	11.855(8)	8.858(4)
c (Å)	15.087(6)	25.632(18)
β (°)	104.63(3)	105.37(2)
U (Å^3)	3747(3)	2540(2)
T (K)	295	295
Z	4	4
D_c (g cm^{-3})	1.47	1.59
$F(000)$	1696	1216
μ(Mo Kα) (cm^{-1})	11.2	13.0
Data collection and reduction		
Crystal dimensions (mm)	0.2×0.3×0.3	0.16×0.75×0.25
Scan width (ω°)	$1.0+\Delta\alpha_1\alpha_2$	$1.0+\Delta\alpha_1\alpha_2$
Total data	6050	5399
Unique data	5334	4492
'Observed' data (N_0)	3959	3184
Observation criterion ($F^2>n\sigma(F^2)$)	2	2
Crystal faces [distance from origin (mm)]	(011)[0.15], (0 $\bar{1}$ $\bar{1}$)[0.15], (0 $\bar{1}$1)[0.12], (01 $\bar{1}$)[0.12], (311)[0.15], ($\bar{1}$ 0 0)[0.2]	(201)[0.083], (20 $\bar{1}$)[0.083], (011)[0.138], (0 $\bar{1}$ $\bar{1}$)[0.138], (0 $\bar{1}$1)[0.125], (01 $\bar{1}$)[0.125], (10 $\bar{2}$)[0.034], ($\bar{1}$02)[0.034]
Transmission coefficient: min., max.	0.742, 0.792	0.788, 0.923
Refinement		
Anisotropic atoms	all non-H	all non-H
Least-squares variables (N_v)	440	329
R[a]	0.047	0.048
R_w[a]	0.048	0.049
S[a]	1.20	1.47
g	0.0004	0.0002
Final difference map features (e Å^{-3})	+0.47, −0.33	+0.48, −0.46

[a] $R=\Sigma|\Delta|/\Sigma|F_o|$; $R_w=[\Sigma w\Delta^2/\Sigma wF_o^2]^{1/2}$; $S=[\Sigma w\Delta^2/(N_o-N_v)]^{1/2}$; $\Delta=F_o-F_c$; $w=[\sigma_c^2(F_o)+gF_o^2]^{-1}$, $\sigma_c^2(F_o)$ = variance in F_o due to counting statistics.

of 25 and 22 centred reflections for **16a**·CH_2Cl_2 and **19**, respectively. In the case of **17**·C_6H_{14} the space group was assigned to be $P2_1/n$ and cell dimensions $a=11.11(1)$, $b=30.08(3)$, $c=10.60(1)$ Å, $\beta=96.9°$ were determined. Although atomic positions for all the atoms were assigned no satisfactory refinement was obtained against the intensity data measured.

For each structure analysis, intensity data were collected by $\omega/2\theta$ scans for unique portions of reciprocal space for $4<2\theta<50°$ and corrected for Lorentz, polarisation, crystal decay (negligible for **19** but *c.* 3% for **16a**·CH_2Cl_2] and long-term intensity fluctuations, on the basis of the intensities of three check reflections repeatedly measured during data collection. For **16a**·CH_2Cl_2 only reflections with intensity above a low threshold were recorded for $40<2\theta<50°$. Corrections for X-ray absorption effects were applied on the basis of the indexed crystal faces and dimensions. The structures were solved by heavy atom (Patterson and difference Fourier) methods, and refined by blocked-cascade least-squares against F.

All hydrogen atoms were constrained to ideal geometries (with C–H = 0.96 Å), except for the hydrogens H(5a), H(5b), H(8a) and H(8b) of **16a**·CH_2Cl_2 and H(7) of **19**. All other atoms were refined without positional constraints. All hydrogen atoms were assigned isotropic displacement parameters, with those of the unconstrained atoms held fixed with U_{iso} at *c.* 1.2 times that of their attached carbon atom.

Final difference syntheses showed no chemically significant features, the largest typically being close to the metal atoms. Refinements converged smoothly to re-

siduals given in Table 5. Tables 6 and 7 report the positional parameters for these structure determinations. See also 'Supplementary material'.

All calculations were made with programs of the SHELXTL [56] system as implemented on a Nicolet R3m/E structure determination system. Complex neutral-atom scattering factors were taken from ref. 57.

TABLE 6. Atomic coordinates ($\times 10^4$) and isotropic thermal parameters ($Å^2 \times 10^3$) for **16a**·CH_2Cl_2

	x	y	z	U^a
Fe(1)	2052(1)	457(1)	325(1)	30(1)*
Fe(2)	2598(1)	313(1)	−1094(1)	33(1)*
P(1)	2549(1)	−1008(1)	1124(1)	36(1)*
P(2)	2969(1)	−1403(1)	−616(1)	38(1)*
P(3)	2973(1)	1216(1)	220(1)	29(1)*
P(4)	1576(1)	1743(1)	−728(1)	34(1)*
C(1)	1846(2)	970(4)	1306(3)	36(2)*
O(1)	1718(2)	1278(3)	1963(2)	60(2)*
C(2)	1476(2)	−531(5)	−245(3)	40(2)*
O(2)	1104(2)	−1197(3)	−607(3)	63(2)*
C(3)	3176(3)	649(5)	−1662(3)	44(2)*
O(3)	3568(2)	878(4)	−2035(3)	70(2)*
C(4)	2014(3)	−330(5)	−1982(4)	47(2)*
O(4)	1637(2)	−715(4)	−2585(3)	80(2)*
C(5)	2084(2)	1811(4)	−1493(3)	40(2)*
C(6)	2043(3)	−2193(4)	1252(4)	57(2)*
C(7)	2978(3)	−809(4)	2313(3)	49(2)*
C(8)	3144(2)	−1661(4)	617(3)	38(2)*
C(9)	2428(3)	−2561(4)	−1079(4)	58(2)*
C(10)	3686(3)	−1913(5)	−903(4)	53(2)*
C(11)	3763(2)	951(4)	1002(3)	35(2)*
C(12)	4244(2)	463(5)	701(4)	52(2)*
C(13)	4840(3)	300(6)	1274(5)	73(3)*
C(14)	4969(3)	654(6)	2155(5)	79(3)*
C(15)	4505(3)	1185(5)	2484(4)	67(2)*
C(16)	3902(3)	1329(4)	1901(3)	49(2)*
C(21)	3097(2)	2752(4)	225(3)	31(2)*
C(22)	3515(3)	3204(4)	−245(4)	47(2)*
C(23)	3685(3)	4324(5)	−157(4)	57(2)*
C(24)	3434(3)	5019(5)	395(4)	57(2)*
C(25)	3012(3)	4597(5)	843(4)	51(2)*
C(26)	2841(2)	3467(4)	761(3)	41(2)*
C(31)	770(2)	1342(4)	−1383(3)	40(2)*
C(32)	583(3)	1300(5)	−2333(4)	49(2)*
C(33)	−35(3)	1029(5)	−2781(4)	70(3)*
C(34)	−473(3)	757(5)	−2303(5)	72(3)*
C(35)	−293(3)	793(6)	−1365(5)	70(3)*
C(36)	319(3)	1087(5)	−915(4)	58(2)*
C(41)	1374(2)	3181(4)	−430(3)	39(2)*
C(42)	1475(3)	4100(4)	−936(4)	47(2)*
C(43)	1272(3)	5175(5)	−765(4)	61(3)*
C(44)	974(3)	5325(5)	−76(4)	63(3)*
C(45)	880(3)	4431(6)	446(4)	65(3)*
C(46)	1073(3)	3364(5)	278(4)	49(2)*
C(50)	250(4)	7847(7)	7322(5)	103(4)*
Cl(1)	−10(1)	7981(2)	6140(2)	119(1)*
Cl(2)	−338(2)	7432(3)	7794(2)	159(2)*

[a]Starred items: equivalent isotropic U defined as one third of the trace of the orthogonalised U_{ij} tensor.

TABLE 7. Atomic coordinates ($\times 10^4$) and isotropic thermal parameters ($Å^2 \times 10^3$) for **19**

	x	y	z	U^a
Fe(1)	1578(1)	1493(1)	788(1)	35(1)*
Fe(2)	1848(1)	4289(1)	1276(1)	32(1)*
P(1)	3227(1)	2685(1)	1174(1)	34(1)*
P(2)	2445(1)	2872(1)	2025(1)	32(1)*
C(1)	2179(5)	−285(6)	678(2)	46(2)*
O(1)	2644(4)	−1398(5)	631(2)	68(2)*
C(2)	1574(4)	2186(6)	124(2)	46(2)*
O(2)	1523(4)	2528(5)	−308(1)	75(2)*
C(3)	−29(5)	1462(6)	634(2)	44(2)*
O(3)	−1051(3)	1417(5)	550(2)	66(2)*
C(4)	327(4)	4438(6)	1308(2)	42(2)*
O(4)	−645(3)	4540(5)	1324(2)	69(2)*
C(5)	2690(4)	5863(6)	1598(2)	43(2)*
O(5)	3289(4)	6836(4)	1808(2)	69(2)*
C(6)	1529(4)	5136(5)	621(2)	40(2)*
O(6)	1301(3)	5694(4)	202(2)	65(2)*
C(7)	3872(4)	2261(6)	1898(2)	38(2)*
C(8)	4411(4)	721(6)	2058(2)	52(2)*
C(11)	4457(4)	3027(6)	869(2)	42(2)*
C(12)	5312(5)	4078(8)	1085(3)	79(3)*
C(13)	6264(6)	4351(9)	862(4)	98(4)*
C(14)	6342(6)	3546(10)	419(3)	88(4)*
C(15)	5495(6)	2496(10)	198(3)	84(3)*
C(16)	4547(5)	2224(8)	416(2)	64(2)*
C(21)	1628(4)	1124(5)	1990(2)	33(2)*
C(22)	1400(4)	428(5)	2441(2)	41(2)*
C(23)	832(4)	−952(6)	2385(2)	50(2)*
C(24)	501(4)	−1624(6)	1884(2)	48(2)*
C(25)	753(4)	−929(5)	1448(2)	41(2)*
C(26)	1314(4)	475(5)	1476(2)	34(2)*
C(31)	2707(4)	3624(5)	2707(2)	37(2)*
C(32)	3484(5)	2913(7)	3141(2)	59(2)*
C(33)	3629(6)	3459(7)	3655(2)	77(3)*
C(34)	3039(6)	4736(8)	3741(3)	76(3)*
C(35)	2291(5)	5459(8)	3318(3)	71(3)*
C(36)	2134(5)	4916(6)	2801(2)	51(2)*

[a]Starred items: equivalent isotropic U defined as one third of the trace of the orthogonalised U_{ij} tensor.

Supplementary material

Full tables of interatomic distances and bond angles, displacement parameters, hydrogen atomic parameters, and observed and calculated structure amplitudes are available from the authors on request.

Acknowledgements

We are grateful to the S.E.R.C. for the award of research studentships (to G.H., K.A.M. and D.A.V.M.) and support, to Dr B. R. Lloyd for synthesising several phosphine ligands and Dr M. Murray for assistance with NMR simulation experiments.

References

1 S. A. R. Knox, *J. Organomet. Chem., 400* (1990) 255.
2 F. A. Cotton and J. M. Troup, *J. Am. Chem. Soc., 96* (1974) 4422.
3 P. A. Wegner, L. F. Evans and J. Haddock, *Inorg. Chem., 14* (1975) 192.
4 R. B. King and K. S. Raghuveer, *Inorg. Chem., 16* (1984) 2482.
5 G. de Leeuw, J. S. Field, R. J. Haines, B. McCulloch, E. Meinjies, C. Monberg, G. M. Oliver, P. Ramdial, C. N. Sampson, B. Sigworth, N. D. Steen and K. G. Moodley, *J. Organomet. Chem., 275* (1984) 99.
6 W. K. Wong, F. W. Chin, G. Wilkinson, M. Motevalli and M. B. Hursthouse, *Polyhedron, 4* (1985) 231.
7 M. G. Newton, R. B. King, M. Chang and J. Gimeno, *J. Am. Chem. Soc., 99* (1977) 2802.
8 G. M. Brown, J. E. Finholt, R. B. King, J. W. Bibber and J. H. Kim, *Inorg. Chem., 21* (1982) 3791.
9 A. L. du Preez, I. L. Marais, R. J. Haines, A. Pidcock and M. Safari, *J. Chem. Soc., Dalton Trans.,* (1981) 1918.
10 R.J. Puddephatt, *Chem. Soc. Rev.,* (1983) 99.
11 B. Chaudret, B. Delavaux and R. Poilblanc, *Coord. Chem. Rev., 86* (1988) 191.
12 G.-Y. Kiel and J. Takats, *Organometallics, 8* (1989) 839.
13 G. Hogarth, F. Kayser, S. A. R. Knox, D. A. V. Morton, A. G. Orpen and M. L. Turner, *J. Chem. Soc., Chem. Commun.,* (1988) 358.
14 G. Hogarth, S. A. R. Knox, B. R. Lloyd, K. A. Macpherson, D. A. V. Morton and A. G. Orpen, *J. Chem. Soc., Chem. Commun.,* (1988) 360.
15 N. J. Grist, G. Hogarth, S. A. R. Knox, B. R. Lloyd, D. A. V. Morton and A. G. Open, *J. Chem. Soc., Chem. Commun.,* (1988) 673.
16 G. Hogarth, S. A. R. Knox and M. L. Turner, *J. Chem. Soc., Chem. Commun.,* (1990) 145.
17 P. E. Garrou, *Chem. Rev., 85* (1985) 171.
18 N. M. Doherty, G. Hogarth, S. A. R. Knox, K. A. Macpherson, F. Melchior and A. G. Orpen, *J. Chem. Soc., Chem. Commun.,* (1986) 540.
19 F. A. Cotton, K. I. Hardcastle and G. A. Rusholme, *J. Coord. Chem., 2* (1973) 217.
20 G. Hogarth, *Ph.D. Thesis,* University of Bristol, UK, 1986.
21 F. A. Cotton, B. E. Hanson, J. D. Jamerson and B. R. Stults, *J. Am. Chem. Soc., 99* (1977) 3239.
22 A. J. Carty, *Adv. Chem. Ser., 196* (1982) 163.
23 D. J. Witter, S. M. Breckenridge, A. A. Cherkas, L. H. Randall, S. A. MacLaughlin, N. J. Taylor and A. J. Carty, *Organometallics, 9* (1990) 2636, and refs. therein.
24 See, for example: R. A. Jones, A. L. Stuart, J. L. Atwood and W. E. Hunter, *Organometallics, 2* (1983) 874.
25 H. H. Karsch, H. F. Klein and H. Schmidbaur, *Angew. Chem., Int. Ed. Engl., 14* (1975) 637.
26 V. C. Gibson, P. D. Grebenik and M. L. H. Green, *J. Chem. Soc., Chem. Commun.,* (1983) 1101.
27 M. Brookhart, K. Cox, F. G. N. Cloke, J. C. Green, M. L. H. Green, P. M. Hare, J. Bashkin, A. F. Derome and P. D. Grebenik, *J. Chem. Soc., Dalton Trans.,* (1985) 423.
28 H. H. Karsch and D. Neugebauer, *Angew. Chem., Int. Ed. Engl, 23* (1983) 127.
29 F. Senocq, M. Basso-Bert, R. Choukroun and D. Gervais, *J. Organomet. Chem., 297* (1985) 155.
30 R. Choukroun and D. Gervais, *J. Organomet. Chem., 266* (1984) C37.
31 N. E. Schore and H. Hope, *J. Am. Chem. Soc., 102* (1980) 4251.
32 Y.-Fu Yu, J. Gallucci and A. Wojcicki, *J. Chem. Soc., Chem. Commun.,* (1984) 653.
33 Y-Fu Yu, A. Wojcicki, M. Calligrais and G. Nardin, *Organometallics, 5* (1986) 47.
34 Y.-Fu Yu, C.-Nin Chau, A. Wojcicki, M. Calligaris, G. Nardin and G. Balducci, *J. Am. Chem. Soc., 106* (1984) 3704.
35 S. Rosenberg, R. R. Whittle and G. L. Geoffroy, *J. Am. Chem. Soc., 106* (1984) 5934.
36 H. Werner and R. Zolk, *J. Organomet. Chem., 303* (1986) 233.
37 H. Werner and R. Zolk, *Organometallics, 4* (1985) 601.
38 P. S. Braterman, R. J. Cross and G. B. Young, *J. Chem. Soc., Dalton Trans.,* (1976) 1310.
39 B. E. Hanson, P. E. Fanwick and J. S. Mancici, *Inorg. Chem., 21* (1982) 3811.
40 D. J. Brauer, S. Hietkamp, H. Sommer and O. Stelzer, *Angew. Chem., Int. Ed. Engl., 23* (1984) 734.
41 V. Riera, M. A. Ruiz, F. Villafane, C. Bois and Y. Jeannin, *J. Organomet. Chem., 375* (1989) C23.
42 F. A. Cotton, J. A. M. Canich, R. L. Luck and K. Idyasager, *Organometallics, 10* (1991) 356.
43 S. Cartwright, J. A. Clucas, R. H. Dawson, D. F. Foster, M. M. Harding and A. K. Smith, *J. Organomet. Chem., 102* (1986) 403.
44 A. R. Quirt and J. S. Martin, *J. Magn. Reson., 5* (1971) 318.
45 H. F. Klein, J. Wenninger and U. Schubert, *Z. Naturforsch., Teil B, 34* (1979) 1391.
46 N. Lugan, J. J. Bonnet and J. A. Ibers, *J. Am. Chem. Soc., 107* (1985) 4484; *Organometallics, 7* (1988) 1538.
47 B. Delavaux, B. Chaudret, F. Dahan and R. Poilblanc, *Organometallics, 4* (1985) 936.
48 J. C. Jeffery, A. G. Orpen, F. G. A. Stone and M. J. Went, *J. Chem. Soc., Dalton Trans.,* (1986) 173.
49 R. W. Hilts, R. A. Franchuk and M. Cowie, *Organometallics, 10* (1991) 1297.
50 D. P. Arnold, M. A. Bennett, M. S. Bilton and G. B. Robertson, *J. Chem. Soc., Chem. Commun.,* (1982) 155.
51 C. S. Kraihanzel and P. K. Maples, *J. Organomet. Chem., 117* (1976) 159.
52 H. H. Karsch and H. Schmidbaur, *Z. Naturforsch., Teil B, 32* (1977) 762.
53 I. Colquhoun and W. McFarlane, *J. Chem. Soc., Dalton Trans.,* (1982) 1915.
54 Z. S. Novikova, A. A. Prishcenko and I. F. Lutsenko, *J. Gen. Chem. USSR, 47* (1977) 707.
55 H. H. Karsch, *Angew. Chem. Int. Ed. Engl., 21* (1982) 311.
56 G. M. Sheldrick, *SHELXTL,* University of Göttingen, FRG, 1985.
57 *International Tables for X-ray Crystallography,* Vol. IV, Kynoch, Birmingham, UK, 1974.